Comparison of Conventional and New Generation Nickel-Titanium Files in Regards to Their Physical Properties

Masaki Tsujimoto, DDS, PhD, Yuu Irifune, DDS,* Yasuhisa Tsujimoto, DDS, PhD,[#] Shizuka Yamada, DDS, PhD,* Ikuya Watanabe, DDS, PhD,[§] and Yoshihiko Hayashi, DDS, PhD**

*Department of Cariology, Nagasaki University Graduate School of Biomedical Sciences, Nagasaki, Japan; [#]Department of Endodontics, Nihon University School of Dentistry at Matsudo, Matsudo, Japan; [§] Department of Dental and Biomedical Materials Science, Nagasaki University Graduate School of Biomedical Sciences, Nagasaki, Japan.

Address requests for reprints to Dr. Yoshihiko Hayashi, Department of Cariology, Nagasaki University Graduate School of Biomedical Sciences, Sakamoto 1-7-1, Nagasaki 852-8588, Japan. E-mail address: hayashi@nagasaki-u.ac.jp

Abstract

Introduction: The aim of this study was to investigate the surface and fractured structure, and physicochemical properties related to cyclic fatigue in various nickel-titanium (Ni-Ti) files. **Methods:** Among a total of 10 groups of Ni-Ti files, conventional Ni-Ti files (Profile and K3) and new-generation Ni-Ti files (Profile Vortex [PV], Vortex Blue [VB], and K3 XF [XF]) with the same tip diameter (ISO size 25) and two types of taper (0.04 and 0.06) were used in this study. Scanning electron microscopy of the file surface structure, differential scanning calorimetry (DSC) and cyclic fatigue resistance tests were conducted. **Results:** Many mechanical grooves were recognized on the file surface. The surface in the Profile group was extremely smooth compared to that observed for the other files. Many shallow hollows besides mechanical grooves were noted on the surface in the XF group. A smooth curve was observed in the Profile, K3 and PV groups. Defined peaks in DSC were observed in the VB and XF groups. The taper 0.04 files exhibited a statistically higher number of cycles to fracture than the taper 0.06 files in all groups (*P*<0.05). Cracks along the mechanical grooves were observed in the Ni-Ti files, with the exception of the XF group. The start of cracking was detected at U-shape sites in the Profile group, the cutting edge in the PV and VB groups and radial islands in the K3 and XF groups. **Conclusions:** The present findings suggest that new-generation Ni-Ti files are not necessarily improved compared to conventional files.

1

Key Words

Cyclic fatigue resistance test, differential scanning calorimetry, heat treatment, Ni-Ti files, scanning electron microscopy

Nickel-titanium (Ni-Ti) files were introduced for root canal treatment by Walia et al. in 1988 (1). Compared to stainless-steel instruments, Ni-Ti files exhibit a high level of corrosion resistance and important properties for increased flexibility and shape memory, characteristics that depend on the temperature, external stress and martensite-type transformation (2). These characteristics allow the materials to endure permanent damage and recover from deformations following as much as 8% strain (2). However, fractures of Ni-Ti files can suddenly occur without preceding signs of permanent deformation and it is of clinical concern that these devices have been reported to display unexpected fracture without warning (3). Ni-Ti files can experience fractures for two reasons: cyclic fatigue and torsional failure (4). Clinically, cyclic fatigue appears to be prevalent in cases of curved root canal treatment (5). Cyclic fatigue is caused by repetitive compressive and tensile stress acting on the outer and inner curves of a file rotating in a curved canal (6). Shear fractures of the material subsequently occur when the maximum strength of the material is exceeded (7). During the manufacture of Ni-Ti instruments, small machining scratches and grooves are invariably left on the surface (8). These surface scratches can serve as notches that concentrate stress, limiting the instrument's lifespan for fatigue (8). Differences exist among endodontists in the U.S. regarding current Ni-Ti instrument use, and expectations for future development are correlated with the level of exposure and training (9).

Ni-Ti files undergo daily development due to improvements in the

production process. For example, there is a new generation of Ni-Ti files, including M-wire (Dentsply Tulsa Dental Specialties [Tulsa, OK]), Blue Technology (Dentsply Tulsa Dental Specialties) and R-phase (SybronEndo [Orange, CA]) devices. Although several reports have indicated that fatigue resistance has not been improved, even in new-generation files (10-12), the differences between new-generation and conventional files with regard to cyclic fatigue conditions have not been fully examined and resolved. The aim of this study was therefore to investigate the characteristics of the intact surface and fractured cross-section structures as well as the physicochemical properties related to cyclic fatigue in various Ni-Ti files. The tested hypothesis was that the new-generation Ni-Ti files materials would be superior in cyclic fatigue resistance compared to conventional materials.

Materials and Methods

Two kinds of Ni-Ti files (Profile [Dentsply Maillefer, Ballaigues, Suisse, abbreviated as PF] and K3 [SybronEndo, Orange, CA]) were selected as conventional superelastic type files. Three kinds of Ni-Ti files (M-wire, Profile Vortex [Dentsply Tulsa Dental Specialties, Tulsa, OK, abbreviated as PV], Vortex Blue [Dentsply Tulsa Dental Specialties, abbreviated as VB] and R-phase, K3 XF [SybronEndo, abbreviated XF]) (13-15) were selected as new-generation files. In total 10 groups of Ni-Ti files with the same tip diameter (ISO size 25) and two types of taper (0.04 and 0.06) were used in this study.

Scanning Electron Microscopy (SEM)

The samples (two unused Ni-Ti files in each group) were mounted on aluminum holders with adhesive carbon tape and observed using an operating microscope (×12.5). After performing the cyclic fatigue test, two fractured files in each group were then examined using a scanning electron microscope (S-3500 N; Hitachi Ltd, Tokyo, Japan). The SEM of the surface, tip and fractured section structures was assessed using a secondary electron image technique, with the instrument operating at 15 kV and a working distance of 15 mm (×150～×2,000 magnification).

Differential Scanning Calorimetry

Differential scanning calorimetry analyses were performed on three unused Ni-Ti files (taper 0.04) from each group. Each specimen measured 3 mm in length derived from the shaft and cut from the instruments using a slow-speed water-cooled diamond saw (Isomet, Buehler, Lake Bluff, IL). The cut specimens were washed in absolute ethanol using ultrasonic cleaner for two minutes and dried at room temperature. The differential scanning calorimetry analyses were conducted (DSC-60, Shimadzu Corp., Kyoto, Japan) over a temperature ranging from -100°C to 100°C using the liquid nitrogen cooling accessory to achieve a subambient temperature. For each analysis, the specimen was first heated from room temperature to 100°C, then cooled from 100°C to -100°C in order to obtain the cooling differential scanning calorimetry curve. The martensitic transformation-starting and transformation-finishing points (M_s, M_f) and

5

reverse austenitic transformation-starting and transformation-finishing points (A_s, A_f) were determined. The values are expressed as the mean $\pm$ standard deviation (SD).

Cyclic Fatigue Resistance Test

The testing device was specially designed for this experiment. The device consisted of a stainless steel base (SUS304) attached to a specifically machined holder that positioned the handpiece (Endo-Mate DT, Nakanishi Inc., Tochigi, Japan) in a precise relationship to the cyclic flexural fatigue testing block. Eight files in each group were tested at 500 rpm (torque 5.0 Ncm) in an artificially curved canal, for a total length of 25 mm, with a 3-mm radius and 60° angle at 10 mm from the canal orifice until instrument fracture was confirmed audio-visually. During the test, the artificial canal was sprayed with oil to reduce the friction of the instrument against the canal wall and minimize the release of heat. The time to instrument separation was recorded with a digital stopwatch, with an accuracy of 0.1 seconds. The total number of cycle to fracture was calculated using the rational speed 500 rpm (8.33 revolutions per second) multiplied by the corresponding time to fracture. The values are expressed as the mean $\pm$ SD. The data were statistically evaluated using the StatView software program (version 5.0; SAS Institute Inc., Cary, NC). Differences were analyzed using a one-way analysis of variance followed by Scheffe's post hoc test at a significance level of $P<0.05$.

6

Results

SEM of the Unused Files

As all the Ni-Ti files used in this study were produced by carving, many mechanical grooves were recognized on the file surface (Fig. 1). The surface in the PF group was extremely smooth compared to that observed for the other files. Many shallow hollows besides mechanical grooves were identified on the surface in the XF group. Furthermore, sticker- and rolled dust-like structures were observed on the file surface, except in the PF group.

Differential Scanning Calorimetry

Fig. 2 and Table 1 show the total heat flow of differential scanning calorimetry for the heating and cooling cycles in addition to the phase transformation temperatures and associated energies of the test specimens. A smooth curve was observed in the PF, K3 and PV groups. Defined peaks (a single peak on cooling, double peaks on heating) were observed in the VB and XF groups. An A_f temperature over 37^oC of was observed in the PV group only.

Cyclic Fatigue Resistance Test

Table 2 shows the data for the number of cycle to fracture. The taper 0.04 files exhibited statistically higher number of cycle to fracture values than the taper 0.06 files in all groups ($P<0.05$). In addition, the PV and VB groups showed statistically higher number of cycle to fracture values

for the taper 0.04 files ($P<0.05$). No statistical difference was observed in the number of cycle to fracture values among the other three groups ($P>0.05$). For the taper 0.06 files, the number of cycle to fracture values in the PF, PV and VB groups were statistically higher than those observed in the K3 and XF groups ($P<0.01$). There were no statistically significant differences between the PF, PV and VB groups or between the K3 and XF groups ($P>0.05$).

SEM of the Fractured Files

Cracks along mechanical grooves were observed in the Ni-Ti files, with the exception of the XF group. In the XF group, no cracks were detected along grinding marks. The start of cracking was detected at U-shape sites in the PF group, the cutting edge in the PV and VB groups and radial islands in the K3 and XF groups.

Discussion

The initiation of fatigue cracks usually occurs at the surface of a working portion of the material. These areas are especially vulnerable if those with the highest levels of stress coincide with the presence of machining marks or miniature grooves (16). Once the cracks are nucleated, their growth progresses slowly and seemingly along these machining grooves, at least initially, until the sudden, final fracture occurs (17, 18). Therefore, the surface observation of the Ni-Ti file material is important prior to conducting a fatigue test. The typical surface structures observed

in the PV, VB and K3 groups are associated with the carving process. Sticker-like structures (19-21) were observed on the surface in the PV, VB, K3 and XF groups. The surface treatment methods used by manufacturers consist of polishing (PV), polishing and thermal (VB), chemical (K3), deoxidation (XF) and electropolishing (PF) techniques. The present SEM analyses showed that these surface treatments after carving influence the surface texture of Ni-Ti files and that the electropolishing (PF) effectively produces a relatively smooth surface without a sticker-like structure. Some manufacturers attempt to remove the machining scratch marks in order to enhance fatigue fracture resistance via such processes as electropolishing (21, 22). Furthermore, as VB group is lower hardness than PV, the titanium oxide formation producing a blue surface color of VB (15) can be used to improve the durability together with the increase of cutting efficiency and corrosion resistance of Ni-Ti file material.

Differential scanning calorimetry provides information for the overall bulk specimen and the effect of temperature changes on the phase transformation (23). The first and second peaks of the heating cycle show the transformation from the martensite phase to the R-phase, and from the R-phase to the austenite phase in differential scanning calorimetry for blue technology files (VB) and R-phase files (XF), respectively. In the present study, the single peak of the cooling cycle indicated the transformation from the austenite to martensite phase in the VB and XF groups. The A_f temperature of the PV material is found to be over 37^oC (body temperature), consistent with the findings of another report (24).

9

The A_f temperature for most conventional superelastic Ni-Ti files is at or below room temperature, whereas that of new controlled memory files, such as PV and VB, is clearly above body temperature. As a result, conventional Ni-Ti files are in the austenite phase during clinical use (25). Martensite phase transformation is associated with excellent damping characteristics due to the energy absorption properties of its twinned phase structure (24). The temperatures of M_s and M_f in the present PV and VB groups demonstrate that the martensite phase appears at normal room conditions. These characteristic phase transformation data of PV and VB well consist with the statistically higher number of cycle to fracture values for the taper 0.04 files.

The performance and mechanical properties of Ni-Ti instruments are influenced by various factors, including the cross-section pattern, flute design, properties of raw materials, and manufacturing processes (26-29). In the present study, the cyclic fatigue resistance test showed significant differences between the instruments. Although flexible files do not generally exhibit resistance against torsional stress, they do show resistance against cyclic fatigue. In contrast, hard files display resistance against torsional stress but do not demonstrate resistance against cyclic stress (30). The present cyclic fatigue resistance test findings showed significant differences between the instruments. For example, the taper 0.06 files with a large cross-section constantly exhibited higher number of cycle to fracture values than the corresponding taper 0.04 files. This means that the larger cross-section file harden and cannot respond

flexibly against cyclic fatigue. Furthermore, another interesting finding is the consistency between the differential scanning calorimetry and number of cycle to fracture data. The differential scanning calorimetry data for the PV and VB groups strongly suggest a high level of fatigue resistance in these groups.

The SEM of the fractured files revealed significant differences with respect to crack and defect sites. This finding suggests that the file design affects the direction and strength of stress. The present study clarified that conventional files have a tendency to develop long crack lines compared to heat-treated files. These electropolishing effects are contradictory to the occurrence of surface defects (31-33). Heat treatment methods, with exception of deoxidization, are therefore concluded to be effective for improving the physical properties of Ni-Ti files.

Conclusion

Many mechanical grooves were recognized on the intact file surface. Cracks along the mechanical grooves were observed in the fractured files, with the exception of the XF group. The PV and VB groups showed statistically higher number of cycle to fracture values for the taper 0.04 files. The R-phase file, XF group exhibited low number of cycle to fracture values. New-generation Ni-Ti files are not necessarily improved compared to conventional files.

Acknowledgements

References

1. Walia HM, Brantley WA. Gerstein H. An initial investigation of the bending and torsional properties of Nitinol root canal files. J Endod 1988;14:346-51.

2. Thompson SA. An overview of nickel-titanium alloys used in dentistry. Int Endod J 2000;33:297-310.

3. West JD, Roane JB, Goerig AC. Cleaning and shaping the root canal system. In: Cohen S, Burns RC. Pathways of the Pulp. 6th ed. St. Louis, MO: Mosby; 1994:206.

4. Setzer FC, Bohme CP. Influence of combined cyclic fatigue and torsional stress on the fracture point of nickel-titanium rotary instruments. J Endod 2013;39:133-7.

5. Kim JY, Cheung GS, Park SH, et al. Effects from cyclic fatigue of nickel-titanium rotary files on torsional resistence. J Endod 2012;38:527-30.

6. Sattapan B, Nervo GJ, Palamara JE, et al. Defects in rotary nickel-titanium files after clinical use. J Endod 2000;26:161-5.

7. Kramkowski TR, Bahcall J. An in vitro comparison of torsional stress and cyclic fatigue resistence of ProFile GT and ProFile GT Series X

rotary nickel-titanium files. J Endod 2009;35:404-7.

8. Xu X, Eng M, Zheng Y, et al. Comparative study of torsional and bending properties for six models of nickel-titanium root canal instruments with different cross-sections. J Endod 2006;32:372-5.

9. Bird DC, Chambers D, Peters OA. Usage parameters of nickel-titanium rotary instruments: a survey of endodontists in the United States. J Endod 2009;35:1193-7.

10. Larsen CM, Watanabe I, Glickman GN, Jianing HE. Cyclic fatigue analysis of a new generation of nickel titanium rotary instruments. J Endod 2009;35:401–3.

11. Gambarini G, Grande NM. Fatigue resistance of engine-driven rotary nickel-titanium instruments produced by new manufacturing methods. J Endod 2008;34:1003–5.

12. Plotino G , Testarelli L. Fatigue resistance of rotary instruments manufactured using different nickel–titanium alloys: a comparative study. Odontology 2014;102:31-5.

13. Al-Hadlaq SMS, AlJarbou FA, AlThumairy RI. Evaluation of cyclic flexural fatigue of M-Wire nickel-titanium rotary instruments. J Endod 2010;36:305-7.

14. Gambarini G, Testarelli L, Galli M, et al. The effect of a new finishing process on the torsional resistance of twisted nickel-titanium rotary instruments. Minerva Stomatol 2010;59:401-6.

15. Gao Y, Gutmann JL, Wilkinson K, et al. Evaluation of the impact of raw materials on the fatigue and mechanical properties of ProFile

Vortex rotary instruments. J Endod 2012;38:398–401.

16. Kim HC, Cheung GS, Lee CJ, et al. Comparison of forces generated during root canal shaping and residual stresses of three nickel-titanium rotary files by using a three-dimensional finite-element analysis. J Endod 2008;34:743-7.

17. Schijve J. *Fatigue of structures and materials*, Dordrecht, The Netherlands: Kluwer Academic; 2001:1-507.

18. Cheung GS, Darvell BW. Fatigue testing of a Ni-Ti rotary instrument: part 2 – fractographic analysis. Int Endod J 2007;40:619-25.

19. Marending M, Lutz F, Barbakow F. Scanning electron microscope appearances of Lightspeed instruments used clinically: a pilot study. Int Endod J 1998;31:57-62.

20. Eggert C, Peters O, Barbakow F. Wear of nickel-titanium Lightspeed instruments evaluated by scanning electron microscopy. J Endod 1999;25:494-7.

21. Anderson ME, Price JW, Paroshos P. Fracture resistance of electropolished rotary nickel-titanium endodontic instruments. J Endod 2007;33:1212-6.

22. Cheung GS, Shen Y, Darvell BW. Does electropolishing improve the low-cycle fatigue behavior of a nickel-titanium instrument in hydrochloride? J Endod 2007;33:1217-21.

23. Brantley WA, Svec TA, Iijima M, et al. Differential scanning calorimetric studies of nickel-titanium rotary endodontic instruments. J Endod 2002;28:567-72.

24. Shen Y, Zhou H-M, Zheng Y-F, et al. Metallurgical characterization of controlled memory wire nickel-titanium rotary instruments. J Endod 2011;37:1566-71.

25. Otsuka K, Wayman CM. *Shape Memory Materials*, 1 st ed. Cambridge, UK: Cambridge University Press; 1998.

26. Tripi TR, Bonaccorso A, Condorelli GG. Cyclic fatigue of different nickel-titanium ensodontic rotary instruments. Oral Surg Oral Med Oral Pathol Oral Radiol Endod 2006;102:e106-14.

27. Johnson E, Lloyd A, Kuttler S, Namerou K. Comparison between a nobel nickel-titanium alloy and 508 Nitinol on the cyclic fatigue life of ProFile 25/.04 rotary instruments. J Endod 2008;34:1406-9.

28. Shen Y, Zhou H-M, Zheng Y-F, et al. Current challenges and concepts of the thermomechanical treatment of nickel-titanium instruments. J Endod 2013;39:163-72.

29. Perez-Higueras JJ, Arias A, de la Macorra JC. Cyclic fatigue resistance of K3, K3XF, and twisted file nickel-titanium files under continuous rotation or reciprocating motion. J Endod 2013;39:1585-8.

30. Peters OA, Paque F. Current developments in rotary root canal instrument technology and clinical use: a review. Quintessence Int 2010;41:479-88.

31. Herold KS, Johnson BR, Wenckus CS. Scanning electron microscopy evaluation of microfractures, deformation and separation in EndoSequence and Profile nickel-titanium rotary files using an extracted molar tooth model. J Endod 2007;33:712-4.

32. Ray JJ, Kirkpatrick TC, Rutledge RE. Cyclic fatigue of EndoSequence and K3 rotary files in a dynamic model. J Endod 2007;33:1212-6.

33. Bui TB, Mitchell JC, Baumgartner JC. Effect of electropolishing ProFile nickel-titanium rotary instruments on cyclic fatigue resistance, torsional resistance, and cutting efficiency. J Endod 2008;34:190-3.

Figure legends

Figure 1. Scanning electron micrographs of unused Ni-Ti file materials. (A) Side view of the file apex. (B) and (C) Side view of the cutting edge and flute of the files.

Figure 2. DSC values for five kinds of Ni-Ti files. The heating and cooling cycles indicate the lower and upper flows, respectively.

Figure 3. Scanning electron micrographs of fractured Ni-Ti file materials. (A) Fractured section. (B) Side view of the fractured edge. (C) Enlargement of the rectangular area in B. The arrows indicate cracks.
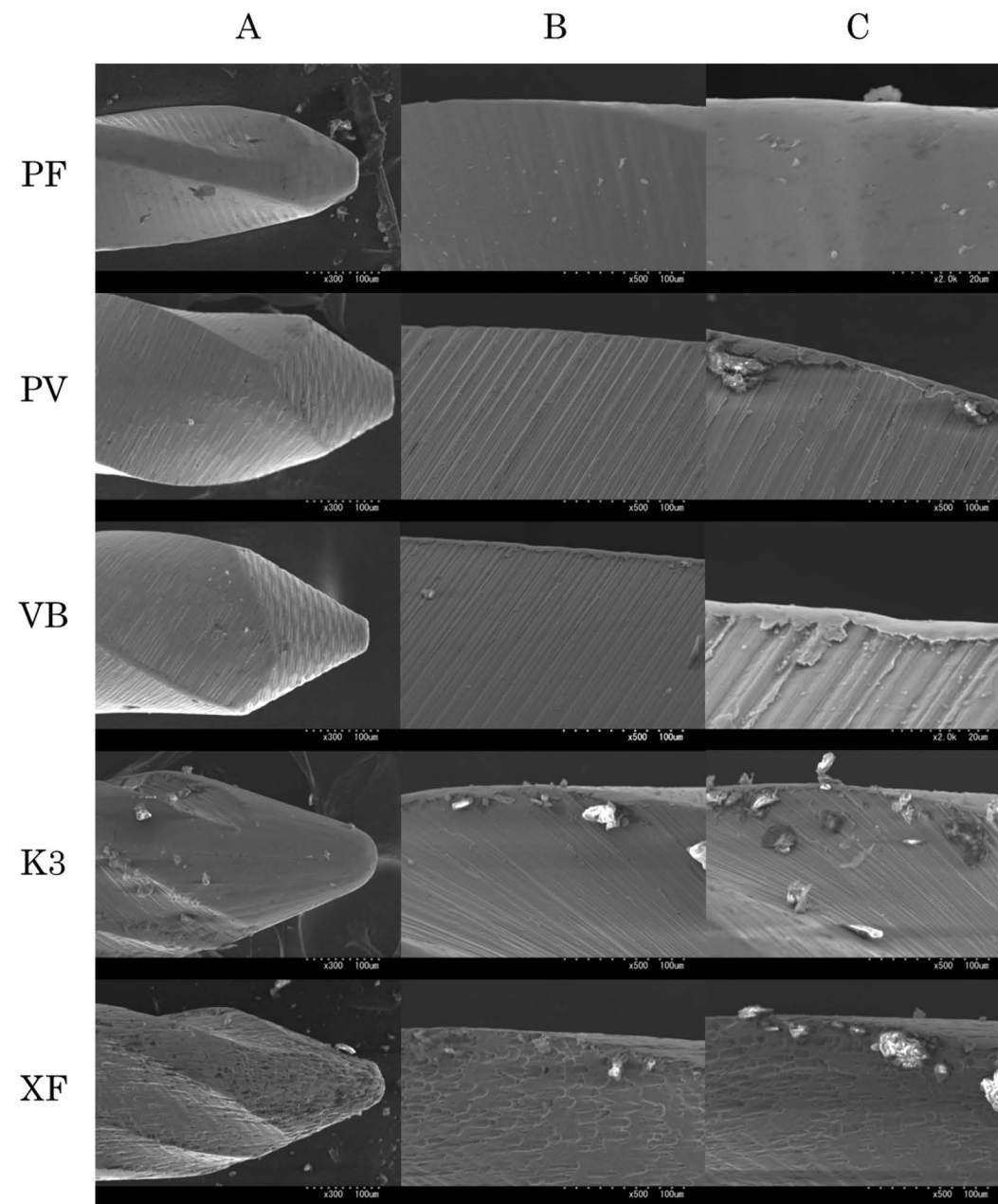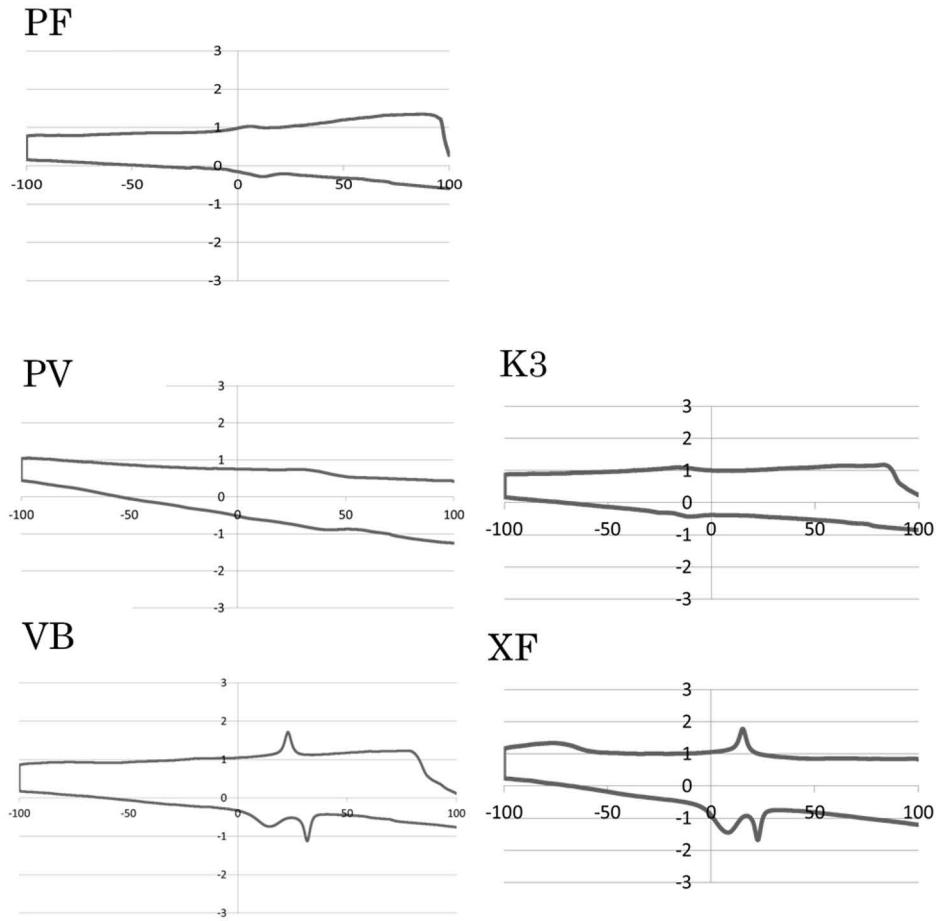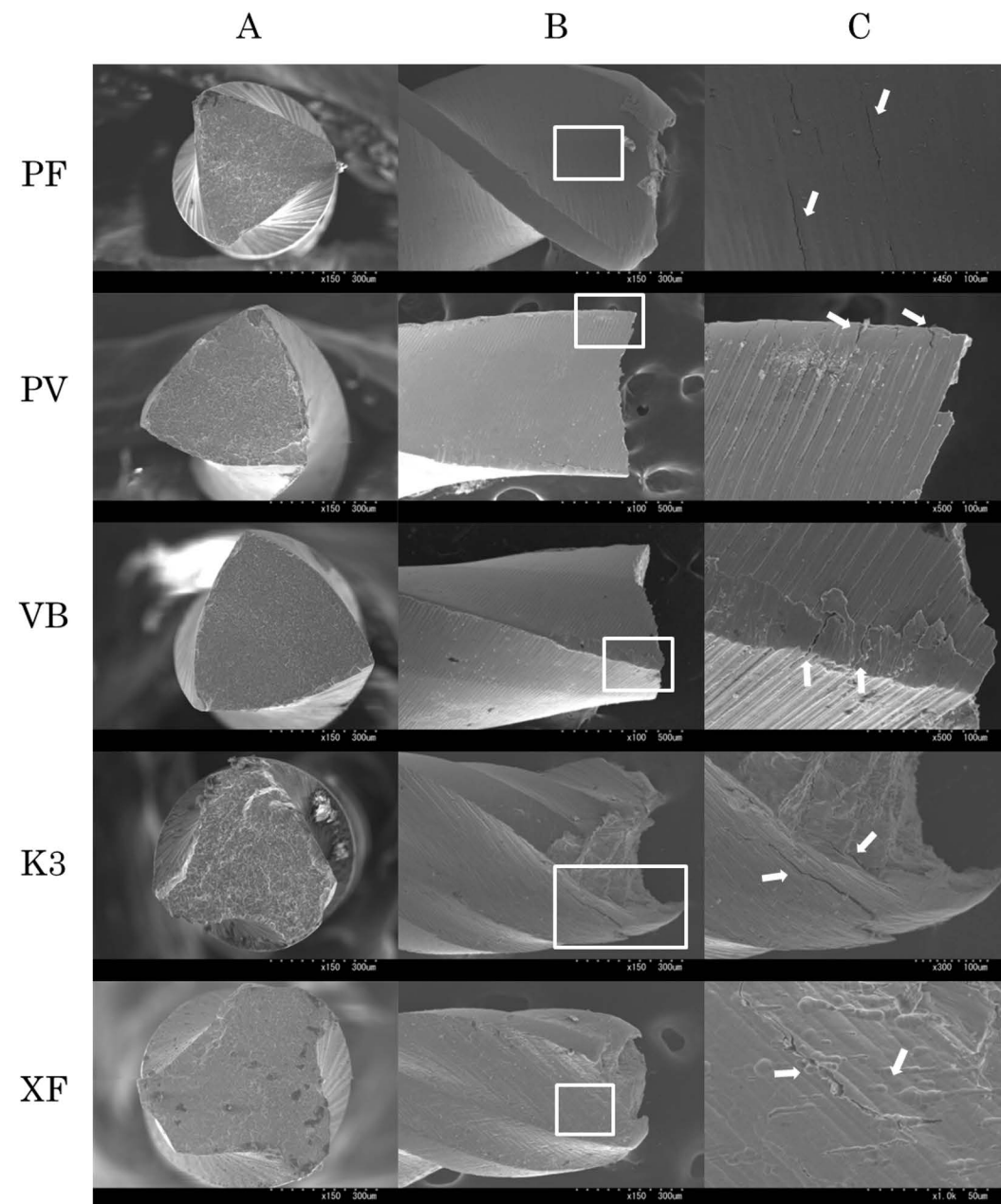
Figure 1.

Figure 2.

PF

PV

K3

VB

XF

Figure 3.

TABLE 1. Temperature and Energy in the Phase Transformation of the Tested NiTi File Materials

Files	Cooling			Heating		
	Ms (℃)	M f (℃)	△H (J/g)	As (℃)	Af (℃)	△H (J/g)
PF	12.85±0.45	-5.04±0.99	1.20±0.19	-23.58±2.29	20.22±1.23	-3.67±0.78
PV	62.08±9.46	3.45±5.91	3.11±0.66	0.08±0.68	53.87±1.52	-3.27±0.39
VB	28.44±1.38	17.73±2.38	2.25±1.02	0.29±0.99	36.93±0.85	-6.77±2.95
K3	-1.60±3.31	-31.90±7.67	1.88±0.59	-25.58±4.55	-2.19±5.72	-2.16±0.82
XF	21.66±2.32	9.31±0.85	3.11±0.26	-4.88±3.22	27.06±1.22	-10.86±1.62

TABLE 2.   Mean Number of Cycle to Fracture and Standard Deviation values for the Various NiTi File Materials

Files	size#25/.04	size#25/.06
PF	665±178.2	515±71.9
PV	903±94.0	509±60.5
VB	909±119.0	565±98.3
K3	606±129.3	296±23.3
XF	741±80.5	297±73.1